ISBN: 978-3-95450-241-7 ISSN: 2673-5350 doi:10.18429/JACoW-IBIC2022-MOP44

NOVEL PHOTOEMISSION TYPE OF X-RAY BEAM POSITION MONITOR FOR THE 'WHITE' UNDULATOR RADIATION*

P. Ilinski†, MAX IV Laboratory, Lund University, Lund, Sweden

Abstract

A novel photoemission type of X-ray Beam Position Monitor (XBPM) for the 'white' undulator radiation is proposed. The XBPM employs beamline frontend fixed mask as a source of photocurrent signal. Signal spatial distribution and XBPM response were analyzed for various undulator radiation parameters.

INTRODUCTION

Photoemission blade type X-ray Beam Position Monitors (XBPM) [1] are standard for most synchrotron radiation facilities. The photoemission blade XBPMs are non-invasive and can provide high spatial resolution but encountering some drawbacks affecting their performance. Initially, the frontend (FE) XBPMs were developed as a standalone component, equipped with positioning stages. Signal response of the photoemission blade XBPM is quite vulnerable to the surface condition of the blades. Also, since operating with negative bias applied to the blade, a conductive deposit can be accumulated at insulator surfaces, leading to substantial increase of the dark current [2]. Operating without bias reduces the blade XBPM signal level.

Most of the time, the FE XBPM is located behind the fixed mask, which is a part of the FE and designed to absorb vast amount of the incident undulator radiation. Knowledge of undulator beam position relative to the FE fixed mask (FM) allows to reduce FM exit aperture and to achieve better beam alignment along the frontend. An XBPM, which is part of the FM was developed [3], it is based on detecting x-ray fluorescence from FM surfaces. Spatial calibration of the XBPM, which is fixed in space, can be performed by deflecting the undulator radiation beam [4]. This is a preferable way to spatially calibrate FE XBPM, since it corresponds to actual operation conditions, when the undulator beam is moving relative to the XBPM and not vice versa.

Proposed novel type of photoemission XBPM is part of the FM. It is detecting the photoemission produced at the FM surface under undulator radiation. The Photoemission Mask (PheM) XBPM will allow to combine XBPM and the frontend FM and to overcome some drawbacks of the photoemission blade XBPMs.

LAYOUT

Photoemission Mask XBPM consists of a fixed mask and detection part with four pickup electrodes, which are hidden from undulator radiation (Fig. 1). The electrodes are collecting photoelectrons emitted from the fixed mask when exposed to the undulator radiation. The PheM XBPM can be a combination of upstream and downstream fixed masks with signal pickup part in between. In this case, the photocurrent signal will be collected from both fixed masks. These signals may be separated in case, if two sets of readout electrodes will be installed in between upstream and downstream masks. The PheM XBPM can also be a combination of upstream mask and downstream readout flange with pickup electrodes, such layout may be compatible with frontends already in operation. Since the fixed masks are electrically grounded, the electrodes need to be under positive potential to collect photoelectrons. In this situation the residual ions will not be attracted to the electrodes and therefore no conductive deposit will be developed at the insulator's surfaces.

Calculation of the PheM XBPM signal distribution was performed for the upstream fixed mask with the exit aperture of 11 mm by 11 mm and the downstream fixed mask with the exit aperture of 9 mm by 9 mm. The upstream fixed mask exit aperture dimensions correspond to the dimensions of the MAX-IV CoSAXS frontend upstream fixed mask. The downstream fixed mask dimensions were chosen not to obstruct the configuration of already installed blade type XBPMs at the CoSAXS frontend. Geometrical and electrostatic layouts can be further optimized for dedicated PheM XBPM design.

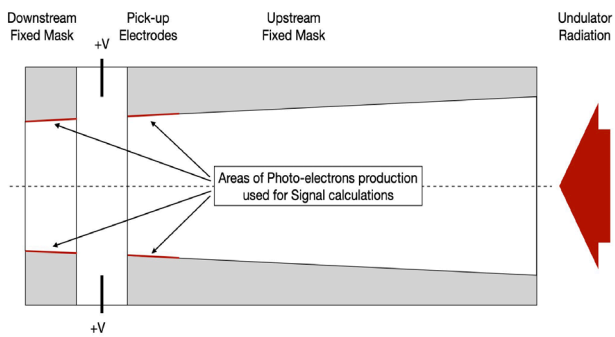

Figure 1: Layout of the Photoemission Mask XBPM.

RADIATION SOURCE

Radiation from planar and elliptical undulator radiation sources was used to calculate the PheM XBPM signal. The flux spectral density of MAX-IV CoSAXS planar undulator for K=1.25 is presented in Fig. 2 for various observation angles. As can be seen, at large observation angles, the PheM XBPM signal is generated mostly by the undulator harmonics with fundamental energies below 1 keV.

The wavelength of fundamental undulator harmonic is proportional to:

*Research conducted at MAX IV is supported by the Swedish Research council (contract 2018-07152), the Swedish Governmental Agency for Innovation Systems (contract 2018-04969), and Formas (contract 2019-02496)
†petr.ilinski@maxiv.lu.se

Content from this work may be used under the terms of the CC BY 4.0 licence (© 2022). Any distribution of this work must maintain attribution to the author(s), title of the work, publisher, and DOI

ISBN: 978-3-95450-241-7 ISSN: 2673-5350 doi:10.18429/JACoW-IBIC2022-MOP44

$$\lambda_n \sim \frac{1}{n}\left(1+\gamma^2\theta^2+\frac{K^2}{2}\right) \quad (1)$$

so, at large observation angles, θ, the wavelength of the fundamental undulator harmonic, λ_n, is dominated by observation angle rather than by undulator K-value. That will make photoelectron signal generated at large angles less dependent to the undulator gap changes.

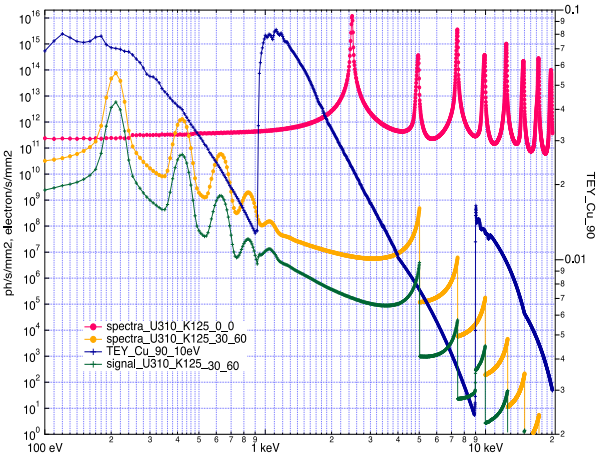

Figure 2: Undulator radiation flux spectral density of MAX-IV CoSAXS planar undulator, K=1.25: on-axis (pink), 0.7 mrad (yellow). Signal spectral density, 0.7 mrad (green). Copper Total Electron Yield (blue).

Bending magnet radiation makes contribution to the total flux and therefore creates a constant background. Modern ultimate storage rings are multi-bent achromats with weak dipoles magnetic field, MAX-IV 3 GeV main dipole has magnetic field of 1.16 T and soft end field of 0.22 T [5]. So, bending magnet radiation will not introduce much of a background signal at MAX-IV 3 GeV storage ring.

SIGNAL

Operation of the PheM XBPM is based on photoemission from the fixed mask under undulator radiation. The resulting photoemission signal is convolution of the undulator spectral density and the total electron yield (TEY) of the FM material, which is mostly copper. Copper TEY data for normal incidence was used [6] in presented signal calculations. The TEY at grazing incidence is higher, so PheM XBPM signal estimations correspond to the lower boundary levels. Signal density spatial distributions were calculated for 300 mA at 10 m for MAX-IV CoSAXS planar undulator for K=1.25 and K=2.0 (Figs. 3-4). Rectangles are indicating photoemission production areas used for signal calculations, outer rectangles correspond to the upstream FM, inner rectangles correspond the downstream FM. Signal density spatial distributions for MAX-IV SoftiMAX APPLE undulator for circular (CP), vertical (VP) and horizontal (HP) polarizations are shown in Figs. 5-7 for K_x=3.35 and K_y=3.35 correspondingly. SRW program was used for undulator radiation calculations [7].

The PheM XBPM signal level is reaching few milli-amperes. The signal levels are higher compared to the blade type XBPM [8] mostly due to the larger area of the photoemission source. Typical area of the XBPM blade is in the order of 1 mm², while photoemission area of the PheM XBPM is ~10 mm². The efficiency of the photocurrent collection by the PheM XBPM will depend on electrostatic field configuration, which can be optimized for required performance.

Sensitivity, linearity and spatial range of XBPM is characterized by the calibration curve. PheM XBPM calibration curves, shown for considered cases in Figs. 8-12, were calculated for vertical direction as (S1-S2)/(S1+S2), where S1 and S2 are signals from the upper and lower fixed masks areas contributing to signal.

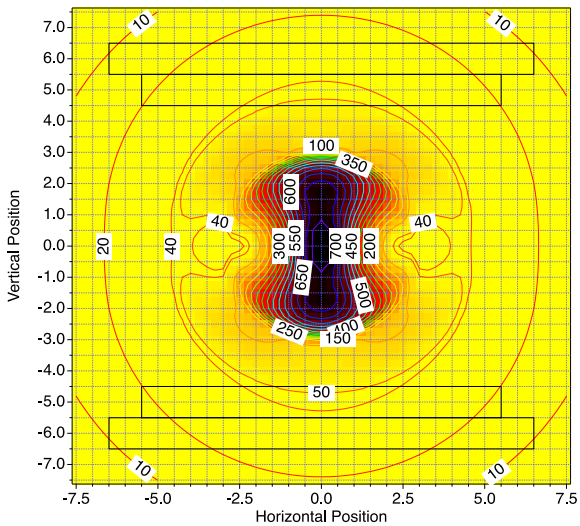

Figure 3: PheM XBPM signal [μA/mm²] spatial distribution at 10 m, MAX-IV CoSAXS planar undulator, K=1.25. Rectangles are indicating photoemission production areas used for signal calculation: upstream FM (outer rectangles), downstream FM (inner rectangles).

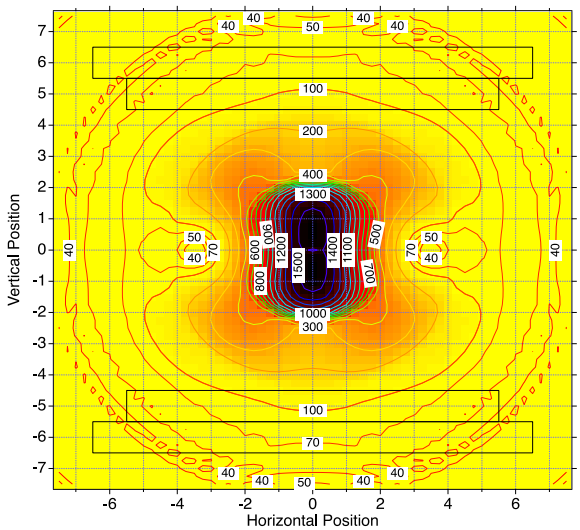

Figure 4: PheM XBPM signal [μA/mm2] spatial distribution at 10 m, MAX-IV CoSAXS planar undulator, K=2.0. Rectangles are indicating photoemission production areas used for signal calculation: upstream FM (outer rectangles), downstream FM (inner rectangles).

Content from this work may be used under the terms of the CC BY 4.0 licence (© 2022). Any distribution of this work must maintain attribution to the author(s), title of the work, publisher, and DOI

ISBN: 978-3-95450-241-7 ISSN: 2673-5350 doi:10.18429/JACoW-IBIC2022-MOP44

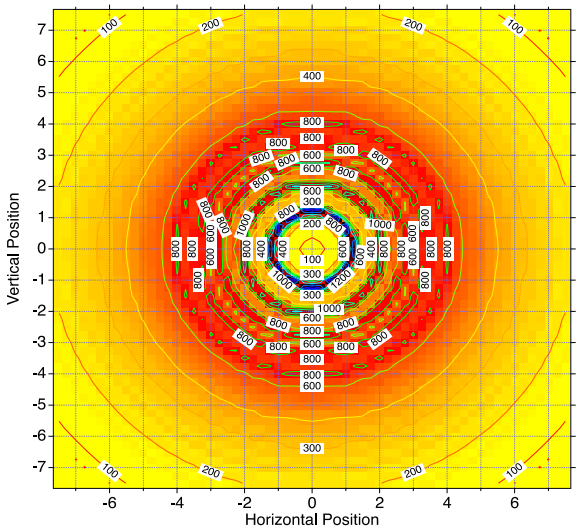

Figure 5: PheM XBPM signal [μA/mm²] spatial distribution at 10 m, MAX-IV SoftiMAX APPLE undulator, circular polarization, K_x=3.35, K_y=3.35.

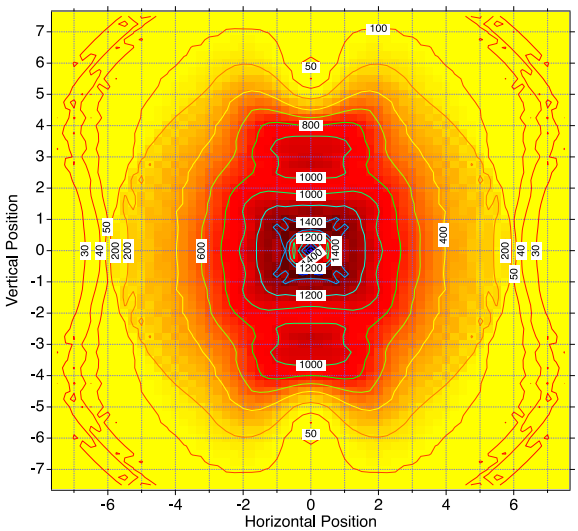

Figure 6: PheM XBPM signal [μA/mm²] spatial distribution at 10 m, MAX-IV SoftiMAX APPLE undulator, vertical polarization, K_y=3.35.

As can be seen, the signal level is higher for the downstream mask (red and blue solid lines) compared to the signal levels from the upstream mask (red and blue dashed lines). Calibration curves were calculated separately for the downstream mask (green solid lines) and for the upstream mask (green dashed lines). In general, signals from both fixed masks, if not separated, will be summed up by the pick-up electrode, the resulting calibration curves are also shown as black solid lines. As can be seen from calibration curves, the PheM XBPM response for considered cases is quite linear up to ~100 urad deviation of the undulator radiation beam. Since there is no high heat load at the detection section, the PheM XBPM spatial range of operation is limited only by the nonlinearity response.

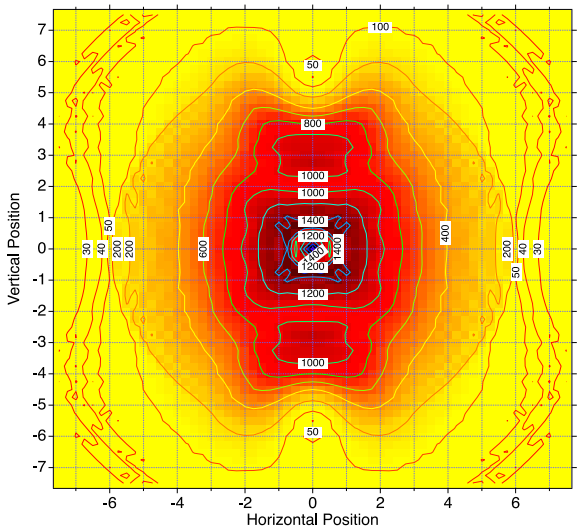

Figure 7: PheM XBPM signal [μA/mm²] spatial distribution at 10 m, MAX-IV SoftiMAX APPLE undulator, horizontal polarization, K_x=3.35.

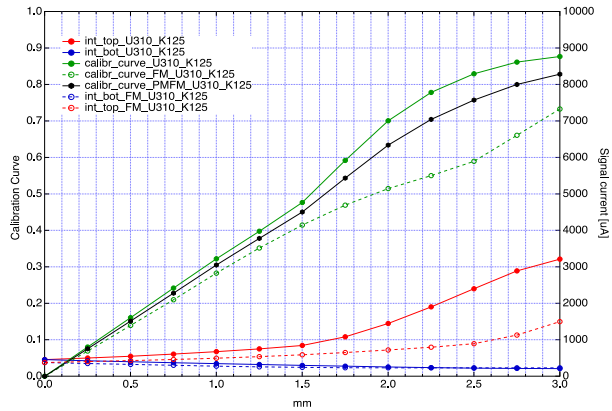

Figure 8: PheM XBPM Signals (red and blue) and Calibration curves (green), total (black), MAX-IV CoSAXS undulator, K=1.25 at 10 m.

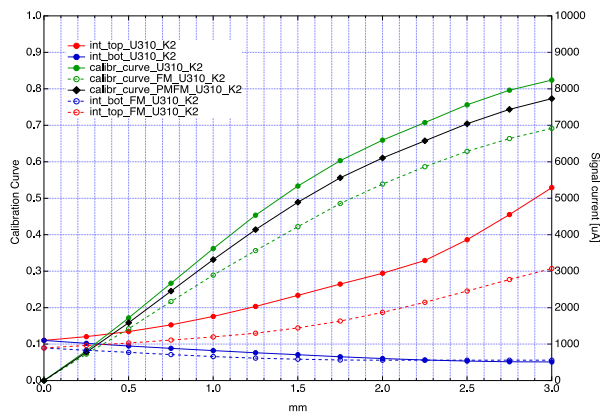

Figure 9: PheM XBPM Signals (red and blue) and Calibration curves (green), total (black), MAX-IV CoSAXS planar undulator, K=2.0 at 10 m.

Content from this work may be used under the terms of the CC BY 4.0 licence (© 2022). Any distribution of this work must maintain attribution to the author(s), title of the work, publisher, and DOI

ISBN: 978-3-95450-241-7 ISSN: 2673-5350 doi:10.18429/JACoW-IBIC2022-MOP44

Content from this work may be used under the terms of the CC BY 4.0 licence (© 2022). Any distribution of this work must maintain attribution to the author(s), title of the work, publisher, and DOI

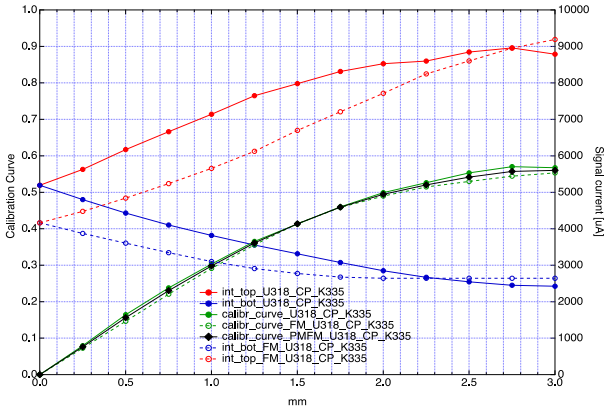

Figure 10: PheM XBPM Signals (red and blue) and Calibration curves (green), total (black), MAX-IV SoftiMAX APPLE undulator, circular polarization, K_x=3.35 K_y=3.35 at 10 m.

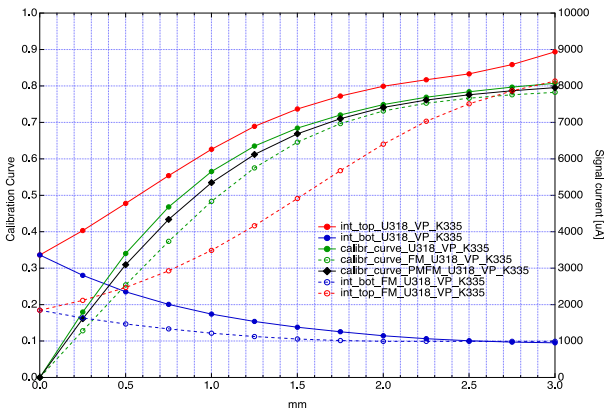

Figure 11: PheM XBPM Signals (red and blue) and Calibration curves (green), total (black), MAX-IV SoftiMAX APPLE undulator, vertical polarization, K_y=3.35, 10 m.

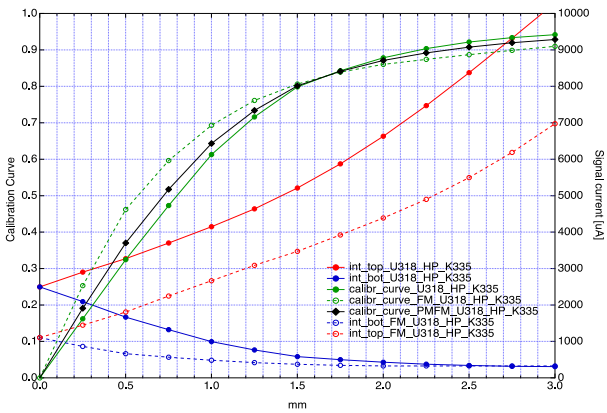

Figure 12: PheM XBPM Signals (red and blue) and Calibration curves (green), total (black), MAX-IV SoftiMAX APPLE undulator, horizontal polarization, K_x=3.35, 10 m.

CONCLUSION

A novel photoemission type of the frontend XBPM for the 'white' undulator radiation is proposed. The PheM XBPM is a part of the frontend fixed mask. Fixed mask is used as a source of photoelectrons, which are collected by positively biased electrodes. Positive bias will eliminate the possibility of building a conductive deposit onto the insulator surfaces around the electrodes. Electrodes are hidden from the undulator radiation, so there is no high heat load at the detection section. The PheM XBPM signal yield are higher compared to the blade type XBPM due to larger area of signal production. Further electrostatic improvements of the PheM XBPM can be consideration of an additional pick-up stage to separate signals from the upstream and the downstream fixed masks, or an additional electrode section in between detection section and the fixed mask to control signals collection.

The PheM XBPM concept will simplify the overall beamline frontend design when directly defining the beam position relative to the frontend fixed mask. Due to the PheM XBPM design simplicity, it can be potentially installed at the existing frontends.

REFERENCES

[1] E. D. Johnson and T. Oversluizen, "Compact flux beam position monitor," *Rev. Sci. Instrum.*, vol. 60, p. 1947. 1989.

[2] C. Bloomer and G. Rehm, "Operation of Diamond Light Source XBPMs with Zero Bias," in *Proc. IBIC2013*, Oxford, UK, Sept. 2013, paper TUPC10, pp. 376-379.

[3] B. X. Yang *et al.*, "Performance Test of the Next Generation X-Ray Beam Position Monitor System for the APS Upgrade", in *Proc. IBIC'16*, Barcelona, Spain, Sep. 2016, pp. 78-81. doi:10.18429/JACoW-IBIC2016-MOPG17

[4] C. Bloomer and G. Rehm, "Real-time Calculation of Scale Factors of X-ray Beam Position Monitors during User Operation", in *Proc. IBIC'12*, Tsukuba, Japan, Oct. 2012, paper MOPA13, pp. 79-82.

[5] H. Tarawneh, L.-J. Lindgren, and B. Anderberg, "Prototype soft end dipole magnet for MAX-IV, fabrication and measurements," *Nucl. Instrum. Methods Phys. Res., Sect. A*, vol. 546, p. 620, 2005.

[6] H. Henneken, F. Scholze, M. Krumrey, and G. Ulm, "Quantum efficiencies of gold and copper photocathodes in the VUV and X-ray range," *Metrologia*, vol. 37, pp. 485-488, 2000.

[7] O. Chubar and P. Elleaume, "Accurate and Efficient Computation of Synchrotron Radiation in the Near Field Region", in *Proc. EPAC1998*, Stockholm, Sweden, June 1998, paper THP01G, p. 1177.

[8] P. Ilinski, "Optimization of NSLS-II Blade X-ray Beam Position Monitors: From Photoemission Type to Diamond Detector", in *Proc. IBIC'13*, Oxford, UK, Sep. 2013, paper MOPC10, pp. 67-70.